



Electro-diffusion of ions in porous electrodes for capacitive extraction of renewable energy from salinity differences

Raúl A. Rica^{a,*}, Roberto Ziano^a, Domenico Salerno^a, Francesco Mantegazza^a,
Martin Z. Bazant^{b,c}, Dorian Brogioli^a

^a Università di Milano-Bicocca, Via Cadore 48, 20052 Monza, Italy

^b Department of Chemical Engineering, Massachusetts Institute of Technology, Cambridge, MA 02139, USA

^c Department of Mathematics, Massachusetts Institute of Technology, Cambridge, MA 02139, USA

ARTICLE INFO

Article history:

Received 5 October 2012

Received in revised form 7 January 2013

Accepted 11 January 2013

Available online 20 January 2013

Keywords:

Salinity differences

Porous electrodes

Super-capacitors

Electrodiffusion

Renewable energy

ABSTRACT

One dimensional theory of the electro-diffusion of ions in activated carbon porous electrodes is applied to describe the dynamic cycle of the capacitive mixing (CAPMIX) based on the double layer expansion (CDLE) technique to harvest renewable energy from salinity gradients. The model combines the electro-diffusion of ions with adsorption and desorption of charge and neutral salt into the double layers at the solid liquid interface, providing a comprehensive and accurate description of the full CAPMIX cycle experimentally measured in prototype cells. A careful analysis of the simulated cycles identifies key parameters for the optimization of the extracted power, like the appropriate thickness and micro-structure of the electrodes, best materials and operation conditions of the electrochemical cell. These directions will be fundamental in the development of this technique as an economically competitive renewable energy source.

© 2013 Elsevier Ltd. All rights reserved.

1. Introduction

It is well known that clean, renewable energy can be extracted from the controlled mixing of waters with different salinities [1–7]. Several approaches have been developed to efficiently harvest the so-called “Blue Energy”, a resource that could be able to globally produce up to 2 TW from the natural mixing of waters occurring in the rivers flowing into the sea [8–10]. Pressure retarded osmosis (PRO) [11–13] utilizes the osmotic pressure difference that develops when a semipermeable membrane (ideally, water-permeable, but salt-impermeable) separates two solutions of different concentration. This pressure difference is used to drive a flow of water from a dilute solution into a more concentrated one, which is converted into electrical power by a turbine and a pressure exchanger. In reverse electrodialysis (RED) [14–16], the two solutions with different salinities are brought into contact through an alternating series of anion and cation exchange membranes combined with two electrodes at each end. The chemical potential difference between salt and freshwater generates a voltage over each membrane and the total potential of the system is the sum of the potential differences over all membranes. These technologies make use of membranes, which are expensive to produce and easily get

fouled and degraded. Moreover, they do not have infinitely high selectivity to the counterion and that they can discharge at high currents, losing selectivity [17].

A novel technique based on the use of electric double layer (EDL) electrochemical capacitors [18–20] has been recently proposed by Brogioli [21], leading to the family of technologies that we now call “capacitive mixing” (CAPMIX) [8]. In CAPMIX, the generation of energy is directly linked to the mixing process, so there is no need for intermediate processes nor conversions, simplifying its implementation and up-scaling. The electrodes of EDL super-capacitors are made of porous activated carbon particles, which are cheap to produce and have long lifetimes. Considering these advantages with respect to other approaches, this technique appears to be a promising way to harvest renewable energy at competitive cost, to be added to the pursued mix of energy sources. Fouling is also an issue in porous electrodes, and much work has to be done in order to minimize its impact. In general, fouling by chemical and biological agents will depend on the local chemistry and biology of rivers, and existing methods to clean membranes and avoid their fast degradation [22] are expected to be also applicable to the maintenance of porous electrodes.

The strategy originally proposed by Brogioli [21,23], called “capacitive energy extraction based on double layer expansion” (CDLE), does not need any membrane, but is based on the dependence of the capacitance of the EDL on the salt concentration. “Capacitive energy extraction based on Donnan potential” (CDP)

* Corresponding author.

E-mail address: rul@ugr.es (R.A. Rica).

combines the CDLE strategy with elements of RED [24,25], incorporating ion-selective membranes to a capacitive cell for charge storage. The inclusion of membranes avoids the need to externally charge the capacitive cell, but adds the aforementioned drawbacks they present. Other recent approaches include the use of ion-selective nanopores to induce current between reservoirs with different salt concentrations [26], useful for portable energy generation devices; or the “mixing entropy battery” (MEB) [27], which is able to extract and store electrochemical energy by selective interactions (faradaic reactions) of their electrodes with ions in solution. MEB does not store charge capacitively, but pseudo-capacitively as chemical energy inside the electrode bulk crystal structure, and uses the dependence of the Nernst potential on salt concentration. Therefore, MEB is in fact a “pseudo-CAPMIX” technique, since the device acts like a “pseudo-capacitor”.

CAPMIX is strongly related to capacitive deionization (CDI) [28,29], a technique that consumes energy to capacitively charge pairs of porous electrodes, thus removing ions from the electrolyte between them. They are not only inverse processes, but it has been shown that, ideally, they can be operated reversibly in order to be thermodynamically equivalent [30,31] and that the same design improvements could lead to optimal performance of both techniques [32].

Although significant advances in the performance of CAPMIX cells have been achieved with simplified models [23,25], an appropriate optimization can be developed only if a full comprehension of all the involved mechanisms is available. Up to now, the bottleneck of CDLE has been the unavoidable presence of charge leakage, i.e., the loss of the stored charge due to undesired surface reactions, that limits the maximum power production [23,25]. We have recently shown that leakage can be almost completely avoided [33], but the development of a competitive technology still requires further advances on the understanding of the properties of the solid/liquid interface, in particular the mechanism responsible for the leakage itself, and guidelines for optimal cell design and operation. Indeed, like in other supercapacitor technologies [18,34,35], the transport of ions inside the porous matrix strongly influences the performance of a CAPMIX cell [36], which has to be taken into account.

Despite the fact that the physical origin of the EDL is easy to understand, its rigorous modeling is far from simple, even in equilibrium conditions [37]. Recent approaches have analyzed the thermodynamic CAPMIX cycle, aiming at the maximization of the extracted energy. The numerical analysis of a modified Poisson–Boltzmann free-energy density functional performed by Boon and van Roij [31] proposes a more efficient cycle than the one tested by Brogioli. More elaborate treatments solve the full set of electrokinetic equations inside a cylindrical pore or use a cell model to describe the EDLs in a highly concentrated plug of carbon particles [38,39]. It is also worthwhile to mention that a continuum description of EDL is not strictly valid inside micropores of size comparable to those of hydrated ions, as confinement effects can lead to very large capacitances inside sub-nanometer micropores [40,41], capacitance oscillations for decreasing pore size [42–44] or different charge storage mechanisms [45]. Moreover, steric effects are typically to be taken into account [46–50], specially under nano-confinement where there appear oscillations in charge density due to ion–ion ordering [51].

In this work, we aim at the description of the kinetics of the CAPMIX cycle, as other studies have previously addressed its thermodynamics. This kinetic description is essential in order to understand the unexpected behavior observed in experiments [21,23,36], and to improve present cell design and operation guidelines of a CAPMIX prototype. Therefore, we avoid a rigorous description of the EDLs and the transport therein, by using a

macroscopic description of them. This description considers charge and salt adsorption into the EDLs as excess quantities that modify the electro-diffusion of ions in the macropores of the electrodes, where the solution is assumed to be electroneutral [52].

The paper is organized as follows. The CDLE principle and its application to Blue Energy harvesting is introduced in Section 2.1, followed by the description of voltage–charge and voltage–concentration relations of the EDL in Section 2.2. Then, the model is completed by the description of a 1D theory of electro-diffusion of ions (Section 2.3). After an overall description of the transport and adsorption phenomena in the porous electrodes (Section 3.1), we discuss some technical details aiming at the maximization of the extracted power from the CAPMIX cycle in Section 3.2.

2. Theory

2.1. The CDLE principle

Consider a parallel plate electrostatic capacitor. In such a device, the voltage difference between the two oppositely charged plates is directly proportional to their separation d according to $V = Q/C_s = Qd/\epsilon$, Q being the charge per unit surface on each plate, C_s the specific (per unit surface) capacitance, and ϵ the electric permittivity of the medium between the plates. We can do work against the electrostatic force on this system by moving apart the two plates. The work thus done is stored by the capacitor as electrostatic energy, increasing the voltage difference between the two plates at constant charge.

As a first approach, the structure of the EDL that forms close to a charged surface in contact with an ionic solution can be thought of as a parallel plate capacitor, where one plate is the solid surface and the other one is the diffuse charge. A measure of the distance between the two plates is given by the Debye length λ_D , that depends on the bulk salt concentration C , as it is the result of a competition between the electrostatic forces that attract counterions to screen the surface charge with the diffusive force trying to equilibrate the concentration of all ionic species [37]. In the case of a monovalent electrolyte ($z_+ = -z_- = z = 1$, being z_{\pm} the valence of cations and anions, respectively), the expression of the Debye length reads:

$$\lambda_D = \sqrt{\frac{\epsilon_r \epsilon_0 k_B T}{2Ce^2}} \quad (1)$$

ϵ_r being the relative electric permittivity of the liquid (typically water), ϵ_0 the electric permittivity of vacuum, k_B is the Boltzmann constant, T is absolute temperature, e is the electron charge and C is expressed in number of ions per unit volume. From this equation, it is clear that the EDL will be thicker the lower the salt concentration, and vice versa. The voltage drop in the diffuse part of the EDL ΔV_D can be described by the Gouy–Chapman surface charge–voltage relationship [37]:

$$\Delta V_D = 2V_T \sinh^{-1} \left(\frac{-Q}{2V_T(\epsilon_r \epsilon_0 / \lambda_D)} \right) \simeq \frac{-Q\lambda_D}{\epsilon_r \epsilon_0} \quad (2)$$

where $V_T = k_B T/e$ is the thermal voltage and Q is the total charge per unit surface in the diffuse part of the EDL. The approximation stands for small surface charge, this limit clearly showing the similarity with a parallel plate capacitor. From Eqs. (1) and (2), we see that the voltage drop in the diffuse part of the double layer increases when C is decreased at constant Q .

By means of an electrochemical cell composed of two electrodes in an electrolyte solution of concentration C_{salt} externally charged with a battery V_{ext} (with an overvoltage close to zero), we can

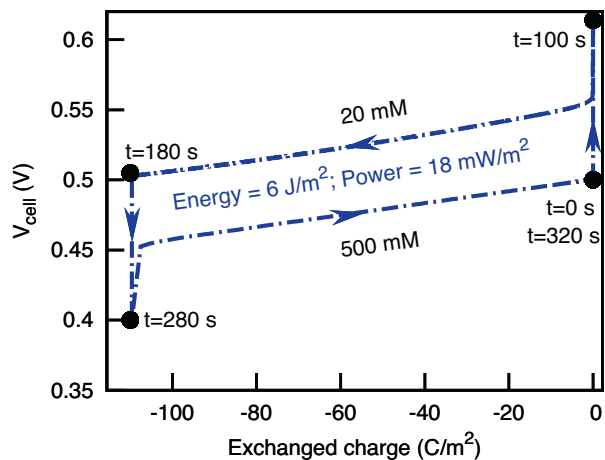


Fig. 1. Simulated CAPMIX cycle in the cell voltage-exchanged charge space. Details of the simulation are like in Fig. 4. The exchanged charge is the charge that is transferred from one electrode to the other in the charge and discharge steps. Note that the zero value of charge has been arbitrarily set to the state of the charged cell.

benefit from CDLE to extract energy from salinity differences performing the following four-step cycle [21], see Fig. 1:

- (i) Exchange the solution with another of lower salt content C_{fresh} at constant stored charge (i.e., setting an open circuit configuration). Upon this exchange, the surface potential will spontaneously increase according to Eq. (2).
- (ii) Discharge the electrodes through an external load $R_{\text{ext,salt}}$ to V_{ext} .
- (iii) Change the electrolyte solution to the one with higher salt content, also at constant charge. Upon this exchange, the surface potential will decrease according to Eq. (2).
- (iv) Charge again the cell though a different external load $R_{\text{ext,fresh}}$ until $V_{\text{cell}} = V_{\text{ext}}$, reaching the initial state and leaving the cell ready for a new cycle.

The energy extracted by this method is the area enclosed in the curve in Fig. 1, and we see that its magnitude depends mainly on the characteristics of the voltage-charge relations at constant salt concentration.

A sketch of the CDLE cell is shown in Fig. 2. Two porous carbon electrodes are placed parallel with a channel in between through which a solution with the desired salt concentration flows. The two electrodes are connected to a voltage supply through a load, here represented by a resistor $R_{\text{ext,fresh}}$ or $R_{\text{ext,salt}}$ [21,23]. Other configurations different from the parallel plate here studied have been proposed for CDP [53,54] and CDI [55,56], but their applicability to CDLE has not been discussed yet.

Since the charge is stored in the EDLs at the interface between the solid and the solution, an efficient CAPMIX cell requires large specific surface allowing for a large charge (hence, energy) storage. EDL super-capacitors present huge specific surfaces (m^2/g or m^2/m^3), allowing the storage of large amounts of ionic charge at the interface between the porous matrix and an ionic solution and a high power output upon discharge. Accordingly, the electrodes are composed of activated carbon porous particles with a characteristic size of the order of a micron that are assembled and glued together with a polymer binder, and present a very large specific surface inside small micropores. The size of the free space between different carbon particles constitutes the macroporosity p_{mA} that will act as pathways for salt and charge transport while the micropores store the ionic charge inside EDLs. The macroporosity is defined as the volume fraction (of the total electrode volume) occupied by the macropores. Similarly, we also define the microporosity p_{mi}

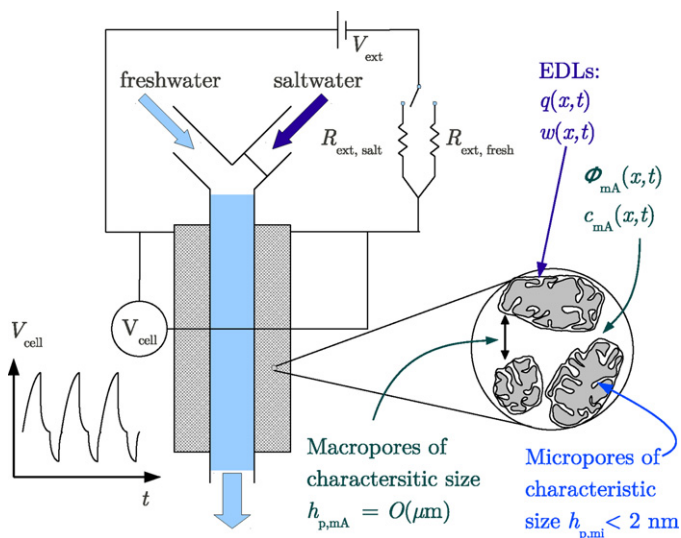


Fig. 2. Sketch of a parallel plate CAPMIX cell. Two electrodes made of assembled micron-sized activated carbon particles are placed parallel and separated by a spacer channel along which a solution of the desired concentration flows. These electrodes are connected to an external circuit composed by a voltage supply and a load, represented by a resistor.

as the volume fraction of the electrode inside the micropores. The characteristic sizes of macro and micro-pores are related to their specific surfaces a_{mA} and a_{mi} (m^2/m^3) of the electrode through $h_{\text{p}} = p_{\text{mA}}/a_{\text{mA}}$ and $h_{\text{p,mi}} = p_{\text{mi}}/a_{\text{mi}}$, respectively [57]. In this work, we will assume that $a_{\text{mA}} \ll a_{\text{mi}}$, hence neglecting the EDLs in the macropores. Moreover, we must point out that such a distinction between microporosity and macroporosity is a simplification, and that in fact it neglects interesting effects such as the observed huge capacitance observed in sub-nanometer pores [40] and the correlation between CDI performance and the fraction of volume occupied by sub-nanometer pores [29].

2.2. Charge-voltage relations in the EDLs: application to CDLE

Our description of the EDL distinguishes between two different regions: the diffuse part of the EDL, described by a Poisson-Boltzmann distribution, and a compact part (Stern layer), where all complications regarding maximum approach of ions to the surface, specific adsorption, discrete charges, surface heterogeneity, etc., reside [37]. However, more realistic models of the diffuse layer can also capture many of such effects [49,58]. Moreover, a description based on the Poisson-Boltzmann distribution will break down at large voltage drops ($\gg V_{\text{T}}$) in the diffuse part of the double layer [49], but the low Stern layer capacitances typical of porous carbon electrodes [59] make the maximum voltages reached in our simulations to be of the order of $2V_{\text{T}}$, thus justifying our assumptions.

The Stern and the diffuse layers are though as a series association of two capacitors, and therefore the total voltage drop across the EDL is obtained as the sum of those at each layer:

$$\Delta V_{\text{EDL}} = \Delta V_{\text{D}} + \Delta V_{\text{St}} \quad (3)$$

where ΔV_{EDL} and ΔV_{St} are the voltage drops of the EDL and of the Stern layer, respectively. In the case of thin EDLs, like those formed in the macropores, these voltage drops are related to the (specific) charge adsorbed by the Gouy-Chapman-Stern (GCS) theory of the EDL. In dimensionless form, Eq. (2) can be written as [52,57]:

$$q_{\text{mA}} = -2\sqrt{c_{\text{mA}}} \sinh \frac{\Delta \phi_{\text{D}}}{2} \quad (4)$$

Here, $q_{mA} = Q/(2e\lambda_D^{\text{salt}}C_{\text{salt}})$ and $c_{mA} = C_{mA}/C_{\text{salt}}$ are the dimensionless charge adsorption per unit surface and salt concentration in the macropore, respectively, with λ_D^{salt} the Debye length when the concentration is C_{salt} . $\Delta\phi_D = \Delta V_D/V_T$ is the dimensionless voltage drop in the diffuse part of the EDL. In the case of a charge-free Stern layer, the charge in the diffuse part of the EDL is related to the voltage drop in the Stern layer through:

$$q_{mA} = -\frac{\Delta\phi_{St}}{\delta_{mA}} \quad (5)$$

where $\Delta\phi_{St} = \Delta V_{St}/V_T$ is the dimensionless voltage drop in the Stern layer. Moreover, $\delta_{mA} = \lambda_{St}/\lambda_D^{\text{salt}}$, λ_{St} being an effective Stern layer thickness. Finally, the amount of salt adsorbed in the EDLs is given by the quantity w_{mA} :

$$w_{mA} = 4\sqrt{c_{mA}} \sinh^2 \frac{\Delta\phi_D}{4} \quad (6)$$

When the thickness of the diffuse part of the EDL is comparable to the characteristic micropore size, overlap between them takes place and the Gouy–Chapman model (Eq. (4)) is not applicable. A way to analyze this effect is to consider the limiting case of Debye length much larger than the pore size ($\lambda_D \gg h_{p,mi}$), a situation likely to occur inside the micropores of porous carbon particles. In this case, we can use the so-called “modified Donnan” model (mD) [57,60–62], which assumes that the electric potential and the concentration of ions inside the micropores are uniform:

$$c_{mi}^{\pm} = c_{mA} \exp(\mp \Delta\phi_D) \quad (7)$$

where $c_{mi}^{\pm} = C_{mi}^{\pm}/C_{\text{salt}}$ are the dimensionless concentrations of cations and anions in the micropores, respectively. The micropore dimensionless charge density $q_{mi} = \frac{1}{2}(c_{mi}^+ - c_{mi}^-)$ leads to the following charge–voltage relation in the micropores, relating the dimensionless voltage drops of the diffuse and Stern layers with the diffuse charge:

$$q_{mi} = -c_{mA} \sinh \Delta\phi_D = -\frac{\Delta\phi_{St}}{\delta_{mi}} \quad (8)$$

with

$$\delta_{mi} = \frac{2eC_{\text{salt}}}{V_T C_{St,vol}} \quad (9)$$

where $C_{St,vol} = C_{St}/h_{p,mi}$ is the volumetric Stern capacity of a micropore. We use $C_{St,vol}$ instead of its surface counterpart C_{St} not only for notation convenience, but also because confining effects make C_{St} be dependent on the pore size and geometry, i.e., the value of $h_{p,mi}$ [40–43]. The salt concentration inside the micropores is defined as

$$w_{mi} = \frac{1}{2}(c_{mi}^+ + c_{mi}^-) = c_{mA} \cosh \Delta\phi_D = c_{mA} + w_{mi}^{\text{excess}} \quad (10)$$

where we have also introduced the dimensionless excess salt adsorption [63]:

$$w_{mi}^{\text{excess}} = c_{mA}(\cosh \Delta\phi_D - 1) = 2c_{mA} \sinh^2 \frac{\Delta\phi_D}{2} \quad (11)$$

Here we see that salt adsorption (w_{mi}^{excess}) is an inherently non-linear process, vanishing at small diffuse layer potentials below V_T .

For intermediate situations between these two limits or when both cases are present, more elaborate models of the EDL are needed, and the full set of electrokinetic equations has to be solved [64]. A very suitable approach is the application of a cell model [38,65,66], widely used in the analysis of concentrated suspensions of colloidal particles and recently used to provide accurate estimations of CDLE performance [39].

2.3. Electro-diffusion in porous electrodes

A charge–voltage relation does not suffice to describe the dynamics of the whole process of energy harvesting via capacitive mixing of river and sea water with porous electrodes. In particular, the charging and discharging processes are not only determined by the RC charging time of the EDL, but the transport of ions in the spacer and inside the porous electrodes is fundamental for the performance and operational issues of the flow cell [52]. As experiments show [21,23,36], different time scales appear during the operation of the CAPMIX cell, revealing complex dynamics in the evolution of the cell voltage and stored charge. To account for these effects, a one dimensional theory for the electro-diffusion of ions in the macropores developed in Refs. [52,57] is used, which provides a good description of the mechanisms taking place. This theory has to be coupled to a proper description of the EDL through a charge–voltage relation, but it is independent of the specific EDL model, i.e., it can be combined with GCS, mD or a cell model.

The treatment is based on the Nernst–Planck equation for point-like ions, thus describing the flux of ions due to gradients of concentration and electric potential. In dimensionless form, this equation relates the reduced ion flux of cations and anions, $j_{\pm} = J_{\pm}/J_{\text{lim}}$, to the gradients of concentration ($\partial c^{\pm}/\partial x$) and electric potential ($\partial\phi/\partial x$) through:

$$j_{\pm} = -\frac{1}{2} \left(\frac{\partial c^{\pm}}{\partial x} \pm c^{\pm} \frac{\partial\phi}{\partial x} \right) \quad (12)$$

where $J_{\text{lim}} = 2D_{mA}C_{\text{salt}}/L_e$ is the diffusion-limited current, $c^{\pm} = C^{\pm}/C_{\text{salt}}$ are the dimensionless concentrations (either in the macropores or in the spacer outside the electrodes) of cations and anions, respectively, ϕ is the dimensionless electrostatic potential ($\phi = V/V_T$, with V the dimensional electric potential), and $x = X/L_e$ is the dimensionless position coordinate, L_e being the thickness of the electrode. D_{mA} is the effective diffusion coefficient of ions inside the macropores of the electrodes.

We distinguish between two regions (see Fig. 3): the stagnant diffusion layer (SDL) ($-L_{\text{SDL}} < X < 0$), i.e., a transition region outside the electrode matrix where the electric potential and the salt concentration change from their values in the bulk to those inside the electrode; and the electrode itself ($0 < X < L_e$), where charge and salt adsorption have to be taken into account. This treatment does not include the transport of ions inside the micropores, which can be relevant in certain conditions [67–69]. However, the present approach has been successfully applied to describe experimental results on capacitive charging of porous electrodes [70], CDI performance [62] and CAPMIX cycles [36]. The good agreement found suggests that the transport in the micropores can be neglected in a first approach, leaving the inclusion of this effect for future work.

Assuming electroneutrality ($c = c_+ = c_-$) and with an appropriate mass balance [52], we obtain the Ohm law and the diffusion equation, describing the electro-diffusion of ions in the SDL, outside the electrode matrix:

$$i_{\text{SDL}} = -c_{\text{SDL}} \frac{\partial\phi_{\text{SDL}}}{\partial x} \quad (13)$$

$$\frac{\partial c_{\text{SDL}}}{\partial t} = d_{\text{SDL}} \frac{\partial^2 c_{\text{SDL}}}{\partial x^2} \quad (14)$$

where i_{SDL} is the dimensionless current density in the SDL (note that it is constant along the whole SDL) and t is the dimensionless time normalized by the characteristic diffusion time inside the porous matrix $\tau_{\text{diff}} = L_e^2/D_{mA}$. Furthermore, $d_{\text{SDL}} = D/D_{mA}$ is the quotient between the bulk diffusion coefficient D and that inside the porous matrix D_{mA} .

While Eqs. (13) and (14) fully describe the transport of ions in the SDL, they have to be modified to account for salt and charge

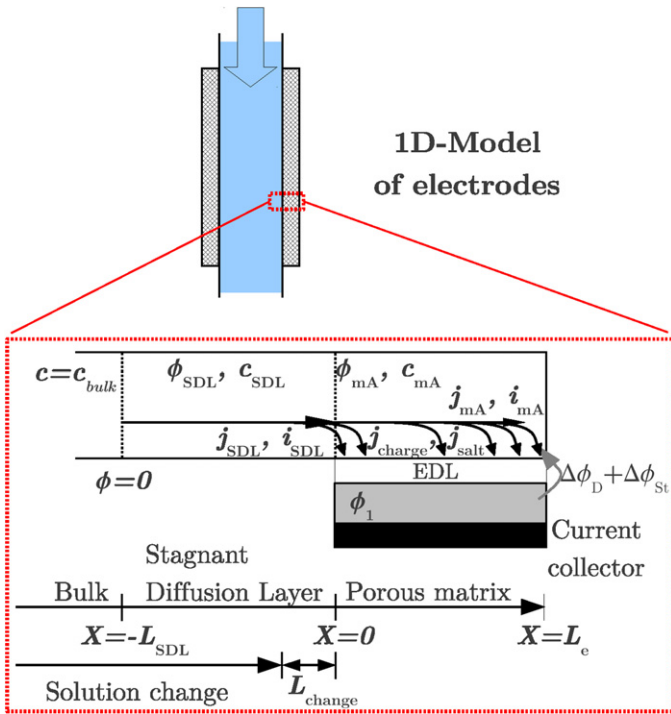


Fig. 3. 1D model of electro-diffusion of ions in porous electrodes applied to CAPMIX. The uniform rates of charge ($i_{\text{SDL}}(t)$) and neutral salt ($j_{\text{SDL}}(t)$) transport in the stagnant diffusion layer (SDL) due to gradients of salt concentration and electric potential are modified inside the porous matrix due to adsorption of both charge ($j_{\text{charge}}(x, t)$) and salt ($j_{\text{salt}}(x, t)$) into the EDLs which form at the solid–liquid interface, leading to position (and time) dependent quantities $i_{\text{mA}}(x, t)$ and $j_{\text{mA}}(x, t)$. The local values of electric potential ($\phi(x, t)$) and salt concentration ($c(x, t)$) determine, together with the adsorbed charge in the EDLs, the (unique) electrode potential through appropriate EDL models. At the beginning of the open circuit steps, the solution in the bulk and in part of the SDL is substituted. The part of the SDL which is not changed instantaneously is determined by the length L_{change} . c_{bulk} is either c_{salt} or c_{fresh} .

adsorption into the EDLs to be valid inside the porous matrix. This modification is obtained performing a volume average for a porous structure of the boundary conditions developed in Ref. [63] to include these effects in the study of the dynamics of blocking parallel-plate electrodes, which describe how charge and salt are adsorbed into the EDLs formed at this interface partially desalting the electrolyte between the electrodes.

Here, we have unified previous treatments, where the opposite limits of thin and thick EDLs have been considered independently. This differentiation is present in [57], where the specific charge and salt adsorption are defined per unit surface in the case of thin EDLs (limit applicable to the EDLs in the macropores), while it is defined per unit volume for thick EDLs (limit applicable to the EDLs inside the micropores). In what follows, we do not make such a distinction, and hence we drop the subscripts in charge and salt adsorption, simply writing q and w , keeping in mind that they are defined per unit surface or per unit volume depending on the considered EDL model (GCS or mD, respectively). For this purpose, we have to introduce a parameter which accounts for the volume available for ions adsorption. Therefore, we define the parameter γ as the volume fraction of electrode occupied by the EDLs. When the Debye length is small as compared with the characteristic pore size and the GC model applies, $\gamma = \lambda_{\text{D}}^{\text{salt}} a$, where a is the surface per unit volume of electrode. The thin double layer approximation implies $\gamma = \lambda_{\text{D}}^{\text{salt}} a \ll p_{\text{mA}}$ [52,57]. On the opposite limit, when we assume that the EDLs are thick as compared to the micropores, the EDLs completely fill the micropores and are strongly overlapped. In this situation, the mD model applies and γ coincides with the microporosity p_{mi} .

The averaging procedure applied to porous electrodes leads to a non-constant current density inside the electrode $i_{\text{mA}} = -c_{\text{mA}} \partial \phi_{\text{mA}} / \partial x$, dependent on the depth x in the electrode, due to the charge adsorption into the EDLs j_{charge} [52,57]:

$$p_{\text{mA}} \frac{\partial i_{\text{mA}}}{\partial x} = -\gamma j_{\text{charge}} = -\gamma \left(\frac{\partial q}{\partial t} \right), \quad (15)$$

The salt transport is also modified by the salt adsorption rate j_{salt} :

$$\frac{\partial c_{\text{mA}}}{\partial t} = d_{\text{SDL}} \frac{\partial^2 c_{\text{mA}}}{\partial x^2} - \frac{\gamma}{p_{\text{mA}}} j_{\text{salt}} = d_{\text{SDL}} \frac{\partial^2 c_{\text{mA}}}{\partial x^2} - \frac{\gamma}{p_{\text{mA}}} \left(\frac{\partial w}{\partial t} \right) \quad (16)$$

Therefore, the transport of ions in the electroneutral macropores is coupled to the reduced adsorbed charge q and salt w into the EDLs, and to the electrode electric potential by the appropriate charge–voltage relations given by the different EDL models.

Eqs. (15) and (16) lead to two coupled PDEs for the concentration of salt in the macropores c_{mA} and the charge stored in the EDLs q as quantities dependent on the depth in the electrode x and time t :

$$\frac{\partial c_{\text{eff}}(x, t)}{\partial t} = p_{\text{mA}} \frac{\partial^2 c_{\text{mA}}(x, t)}{\partial x^2} \quad (17)$$

$$\gamma \frac{\partial q(x, t)}{\partial t} = p_{\text{mA}} \frac{\partial}{\partial x} \left(c_{\text{mA}} \frac{\partial \phi(x, t)}{\partial x} \right) \quad (18)$$

where

$$c_{\text{eff}}(x, t) = p_{\text{mA}} c_{\text{mA}}(x, t) + \gamma w(x, t) \quad (19)$$

is an effective salt concentration, defined as total number of ions inside pores and EDLs per unit total electrode.

The boundary conditions between the two regions are as follows. At the interface between the SDL and the electrode ($X=0$), we have continuity in concentration $c_{\text{SDL}} = c_{\text{mA}} = c_0$ and electric potential $\phi_{\text{SDL}} = \phi_{\text{mA}} = \phi_0$. The current i on either side is the same but for the macroporosity p_{mA} correction, thus, $i_{\text{SDL}} = p_{\text{mA}} i_{\text{mA}}$. Similarly, we have continuity in salt flux, $d_{\text{SDL}} \frac{\partial c}{\partial x} |_{\text{SDL}} = p_{\text{mA}} \frac{\partial c}{\partial x} |_{\text{mA}}$. At the outer boundary of the SDL ($X = -L_{\text{SDL}}$), in contact with the bulk solution, we have $c = c_{\text{bulk}}$ and $\phi = 0$. The inner boundary of the electrode ($X = L_e$) is assumed to be blocking for all ions: $\frac{\partial c_{\text{mA}}}{\partial x} = 0$ and $i_{\text{mA}} = 0$.

In order to couple the dynamics of the cell with the external circuit (composed by the cell in series with the external source V_{ext} and a resistor R_{ext}), we impose the continuity of the current inside the cell and in the external circuit:

$$I_{\text{ext}} = \frac{V_{\text{cell}} - V_{\text{ext}}}{R_{\text{ext}}} = i_{\text{SDL}} \frac{2C_{\text{salt}} eDA}{L_e} \quad (20)$$

where A is the geometric surface of the electrodes.

In our simulations, the salinity change steps (performed in open circuit, $I_{\text{ext}} = 0$), are done by instantaneously substituting the solution in part of the SDL, leaving the solution unchanged in a layer close to the electrode of thickness L_{change} (see Fig. 3). In this work, we arbitrarily set its value to $L_{\text{change}} = 20 \mu\text{m}$.

The cell voltage, defined as the voltage difference between two identical but oppositely charged electrodes, is calculated at each time step from the value of the electrode potential ϕ_1 defined with respect to the potential at boundary between the SDL and the bulk, see Fig. 3. We will simulate only one electrode, so the cell voltage is:

$$V_{\text{cell}} = 2\phi_1 V_{\text{T}} - \Delta V_{\text{int}} \quad (21)$$

where ΔV_{int} is the voltage drop in the internal resistance (see Fig. 4) and ϕ_1 can be obtained from the macropore potential and the voltage drop of the EDL at $x=0$, $\phi_1 = \phi_{\text{mA}}(x=0) + \Delta\phi_{\text{D}}(x=0) + \Delta\phi_{\text{St}}(x=0)$. The internal resistance has two origins, namely, the resistivity of the solution in the spacer

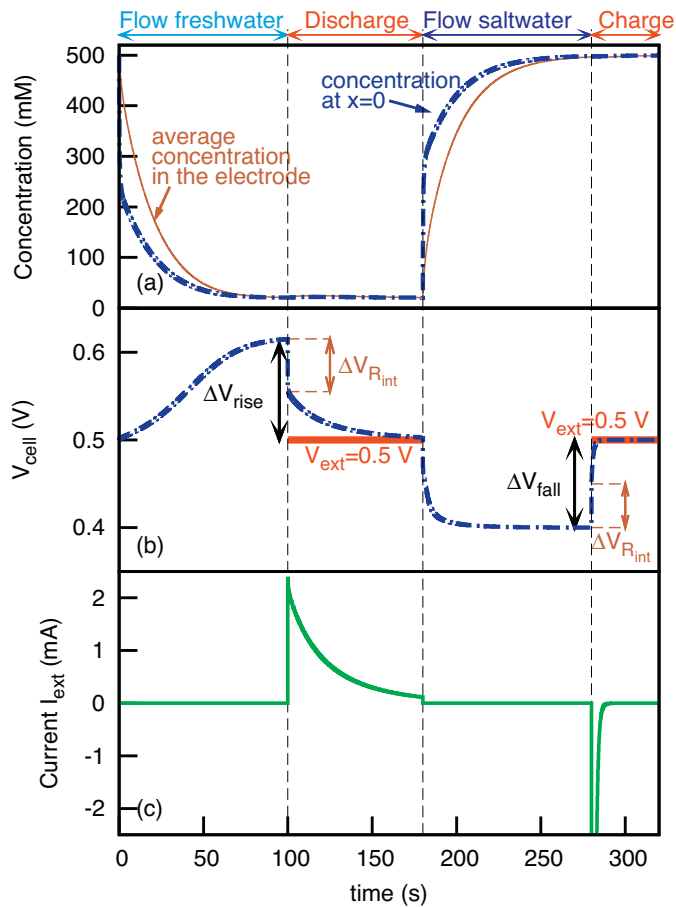


Fig. 4. Evolution of the concentration of salt in the electroneutral macropores of the electrodes (a), cell voltage (b) and current in the external circuit (c) during a CAPMIX cycle. Thick red lines in (b) indicate when the cell is connected to the external source $V_{ext} = 500$ mV. Parameters of the calculation: $A = 1.5$ cm \times 1.5 cm; $L_e = L_{SDL} = 150$ μ m; $d = 1$ mm; $C_{St,vol} = 0.1$ GF/m³; $p_{mi} = p_{mA} = 0.3$; $R_{ext,fresh} = 25$ Ω ; $R_{ext,salt} = 1$ Ω . (For interpretation of the references to color in this figure legend, the reader is referred to the web version of this article.)

between the electrodes (but not that inside the macropores of the porous matrix) and the resistivity of the carbon itself. In general, the resistivity of the carbon is much smaller than that of the electrolyte, and will be neglected in this work. Therefore, in our simulations, the internal resistance is calculated at each time as the resistance of the solution in the spacer between the two electrodes.

Eqs. (17) and (18), coupled with the external circuit given by Eq. (20), make a strongly non-linear system which cannot be solved analytically, although some approximations allow to identify different dynamical regimes [52,57]. As we are interested on the full description of a CAPMIX experiment, we perform the full numerical solution in the four steps cycle, as shown in the next section.

3. Results and discussion

3.1. Overall behavior

We consider a cell composed by two electrodes with geometric area $A = 1.5$ cm \times 1.5 cm and thickness $L_e = 150$ μ m, placed parallel and opposite to one another at a distance $d = 1$ mm (see Fig. 2). As in previous works [36,52,57], we also assume $L_{SDL} = L_e$. The electrodes are characterized by a Stern layer capacitance per unit volume $C_{St,vol} = 0.1$ GF/m³ and porosities $p_{mi} = p_{mA} = 0.3$.

The cell is initially charged to $V_{ext} = 500$ mV in a 500 mM NaCl solution, and then the CAPMIX cycle starts. Fig. 4(a) depicts how

the average concentration inside the electrode (i.e., the average of $c_{mA}(X)$ between $X=0$ and $X=L_e$) and the concentration at the interface between the electrode and the SDL change with time. The evolution of the cell potential and the external current solution during the four-steps CAPMIX cycle are shown in Fig. 4(b) and (c), respectively. In the first step of the cycle, the salt solution between the electrodes is substituted by freshwater in open circuit ($I_{ext} = 0$). Due to the low salt concentration in this region, the salt inside the porous matrix diffuses out by the salinity gradient until it is canceled, leading to the expansion of the EDLs at the carbon/solution interfaces and to the increase in the cell voltage, as shown in Fig. 4(b). Once the cell voltage saturates reaching a plateau, the cell is discharged to the external source through an external load $R_{ext,fresh} = 25$ Ω . After the cell voltage equals that of the external source, we flow again saltwater between the two electrodes. The salt now diffuses from the inter-electrode space to the porous matrix, contracting the EDLs and decreasing the cell potential. Finally the cell is charged to the external source through a load $R_{ext,salt} = 1$ Ω , leaving it ready to start a new cycle. The discontinuity on the cell voltage $\Delta V_{R_{int}}$ seen at the beginning of the discharge and charge steps is due to the discontinuity in the current through the cell when the circuit is closed.

Strikingly, in agreement with previous experiments [21,23,36], the model predicts that the characteristic rise time (switch from saltwater to freshwater) is much longer than the characteristic fall time (fresh to salt) and also much longer than the characteristic time of the diffusion inside the macropores of the electrode. This happens even if, as in the shown case, salination and desalination due to charge and salt adsorption into the EDLs are not important enough to make both diffusion processes asymmetric. In particular, it is impressive to see that while after 1 s the concentration at the electrode–solution interface has fallen to less than half its value, the cell voltage remains almost unaltered, see Fig. 4(b).

In order to study the time response, we evaluate the characteristic single exponential time of rise τ_{rise} and fall τ_{fall} in the solution change steps; i.e., we evaluate the time needed by the cell voltage to reach the value $V_{cell} = (1 - \exp(-1))V_{cell,max}$, being $V_{cell,max} = V_{ext} + \Delta V_{rise}$ (see Fig. 4(b)) the cell voltage at which it saturates. In the same way, τ_{fall} is defined as the time needed to decrease the cell potential from $V_{cell} = V_{ext}$ to $V_{cell} = (1 + \exp(-1))V_{cell,min}$, with $V_{cell,min} = V_{ext} - \Delta V_{fall}$. The characteristic times of the simulation in Fig. 4(b) are $\tau_{rise} \approx 50$ s and $\tau_{fall} \approx 3$ s ($\tau_{rise}/\tau_{fall} \approx 20$), while the characteristic diffusion time can be estimated to be $\tau_{diff} = L_e^2/D_{mA} \approx 15$ s.

This asymmetry between the two open circuit transients (the characteristic times needed by the cell voltage to stabilize when we switch from salt- to fresh water, and vice versa) is mainly due to the highly non-linear voltage–concentration relation predicted by the EDL models [36]. Consider a constant charge curve in the V_{cell} –concentration space (solid and dashed lines in Fig. 5). When the concentration is above 200 mM, the voltage changes very little with concentration, while below that value the dependence is very strong. Therefore, we need to decrease the concentration of the solution below 200 mM when we switch from salt to freshwater to see a significant effect on the cell voltage, while the decrease in voltage in the opposite step (fresh to salt) is faster.

Another mechanism contributing to the asymmetry can be also observed in Fig. 5, which also depicts the path followed by the cell in the voltage–concentration space (dashed-dotted line). It is interesting to see that this path does not follow a constant charge evolution in the open circuit steps (none of the solid or dashed lines), but a more complex one. In particular, the evolution of the voltage with the concentration is slower at the beginning of the switching steps (i) and (iii) than the predicted by constant-charge paths. This is due to a redistribution of the charge along the depth X in the electrode,

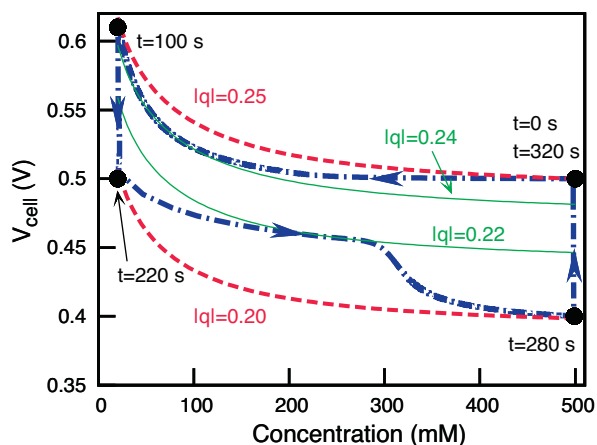


Fig. 5. Dashed-dotted line: CAPMIX cycle in Fig. 4, showing the evolution of the cell voltage with the salt concentration at $x=0$, which does not follow any $q = \text{constant}$ line. Solid and dashed lines: cell voltage vs salt concentration for the indicated values of charge concentration in the micropores. Black dots indicate the positions of the first point of each step, starting at the indicated time.

although the total charge in the electrode is kept constant [36]. This mechanism takes place in each electrode individually, while no current flows through the external circuit.

The origin of this behavior can be understood from a local description of the dynamics of adsorption of charge and salt into the EDLs, as it is done in Fig. 6. Here we represent the time evolution of the position-dependent salt concentration in the SDL ($x \in [-1, 0]$) and in the (transport) macropores inside the electrode ($x \in [0, 1]$), together with the volume densities inside the micropores ($x \in [0, 1]$) of charge ($q(x, t)$) and salt adsorption ($w^{\text{excess}}(x, t)$).

The discharge/charge steps do not show new phenomenology, as these steps have been previously analyzed [52,57]. During these processes, charge and salt are released/adsorbed to/from the EDLs, partially salting/desalting the solution locally. As the considered external voltage is not too high and a CAPMIX cycle only implies small variations of the EDL potential drop around it, the impact of salination/desalination on the global performance of the cell here considered can be neglected. However, these effects are important for the comparison with experimental data, when the cell is finite and the concentration of the bulk can be modified during the cycle.

On the other hand, the open circuit steps present very rich phenomenology, appearing transport mechanisms with different time scales (others than the simple diffusion of salt). After the instantaneous change of the solution from salt to fresh in the bulk and in part of the SDL ($X \in [-L_{\text{SDL}}, -L_{\text{change}}]$), diffusion transports salt from the highly concentrated macropores toward the fresh solution, thus establishing a concentration gradient inside the porous matrix (quite sharp at short times after the switching, $\tau \simeq L_{\text{change}}^2/D \leq 1$ s, smoothing out at larger time scales).

Within this short time scale, a redistribution of the charge in the micropores along the depth of the electrode occurs: a current inside each individual electrode transports counterions from the surface micropores toward those deeper in the electrode. This current is responsible for the transition observed in Fig. 5 from the $q = 0.25$ to the $q = 0.24$ curves. This redistribution of counterions is more apparent in step (iii), when the current carries the counterions in the opposite direction, increasing its density in the micropores closer to the SDL–electrode interface ($x=0$), and inducing the transition between the curves $q = 0.20$ and $q = 0.22$ in Fig. 5.

In both open circuit steps, the redistribution of counterions is driven by the appearance of an electric field. This is due to the gradient of concentration that is established in the macropores of the electrode when we change the solution in the cell: due to

the CDLE principle, a local variation of salt concentration modifies the local electric potential of the solution and the carbon, which react sustaining currents (of counterions in the solution, electrons in the carbon) to cancel the gradients. If the open circuit step is long enough to reach a constant salt concentration along the electrode, new currents appear in the opposite direction, and the uniform distribution of counterions is recovered [36]. Note that, in spite of similarities, this process is different from the redistribution of charge which occurs along a single micropore when transport inside them becomes important (at longer time scales) [67].

In both cases, the charge redistribution slows down the dynamics of the system, as it is clearly seen if we carefully analyze Fig. 5. Here we see that the path followed by the cell in the voltage–concentration space (thick dashed dotted line) is flatter at the beginning of the solution change (salt-to-freshwater at high charge, fresh-to-saltwater at low charge) than the constant charge paths (solid and dashed lines). However, the electrode relaxes to a uniform charge distribution faster in the fresh-to-salt step because in this step there is less charge to be transferred, so the characteristic time is necessarily shorter.

If longer electrodes than the considered here are to be studied, charge redistribution will also appear the electrodes along the direction of the flow during the solution change steps, as gradients of electrolyte concentration will also develop in this direction. Accurate modeling of this situation requires a two-dimensional treatment, which is out of the scope of the present work.

Another interesting effect observed during salinity change in open circuit is the effect on the adsorbed salt into the EDLs: the salt adsorption w^{excess} increases when salt concentration is decreased, and vice versa. Therefore, desalination of the macropores by an increase on salt adsorption from micropores takes place when we change from salt to freshwater due to salt adsorption (without changing the amount of stored charge q), while the opposite (salination) happens when switching from fresh to saltwater. This effect was already noticed in [71], where the authors observed that the charge efficiency, defined as the adsorbed salt per unit charge, increases when decreasing the bulk salt concentration.

3.2. Toward optimization

In this section, we present trends of some key parameters that could improve the power extraction in a CAPMIX cell. These results are complementary to other studies focused on the maximization of the extracted energy [31,39], and would have to be considered together with them in the design of an optimal CAPMIX cell.

It is clear that the power generation will be improved by a reduction of the duration of every step of the cycle. As we have already seen, the longest steps are those performed with freshwater, so special attention has to be paid to shorten these if increased cycle power is desired. On the one hand, the discharge step can be performed at constant current instead of discharging the cell to a constant external voltage, thus optimizing the extracted power during this step thanks to better impedance matching [25,27]. On the other hand, the shortening of the switching step can be done by a proper design of the CAPMIX cell.

The dependence of the characteristic times with the thickness of the electrodes is illustrated in Fig. 7, where the expected quadratic behavior is clearly observed. Therefore, a fast response requires thin electrodes. From this quadratic behavior, an effective diffusion coefficient D_{eff} can be obtained, fitting the data to an equation of the form $\tau = \tau_0 + L_e^2/D_{\text{eff}}$. Two different values are obtained, depending on the considered data set (τ_{rise} or τ_{fall}), which differ in one order of magnitude ($D_{\text{eff}}^{\text{rise}} = 8.7 \times 10^{-10} \text{ m}^2/\text{s}$ and $D_{\text{eff}}^{\text{fall}} = 9.7 \times 10^{-9} \text{ m}^2/\text{s}$). They are also different from the average diffusion coefficient of NaCl ($D_{\text{NaCl}} = 1.6 \times 10^{-9} \text{ m}^2/\text{s}$). This apparent discrepancy is expected from the fact that we do not directly measure the diffusion, but

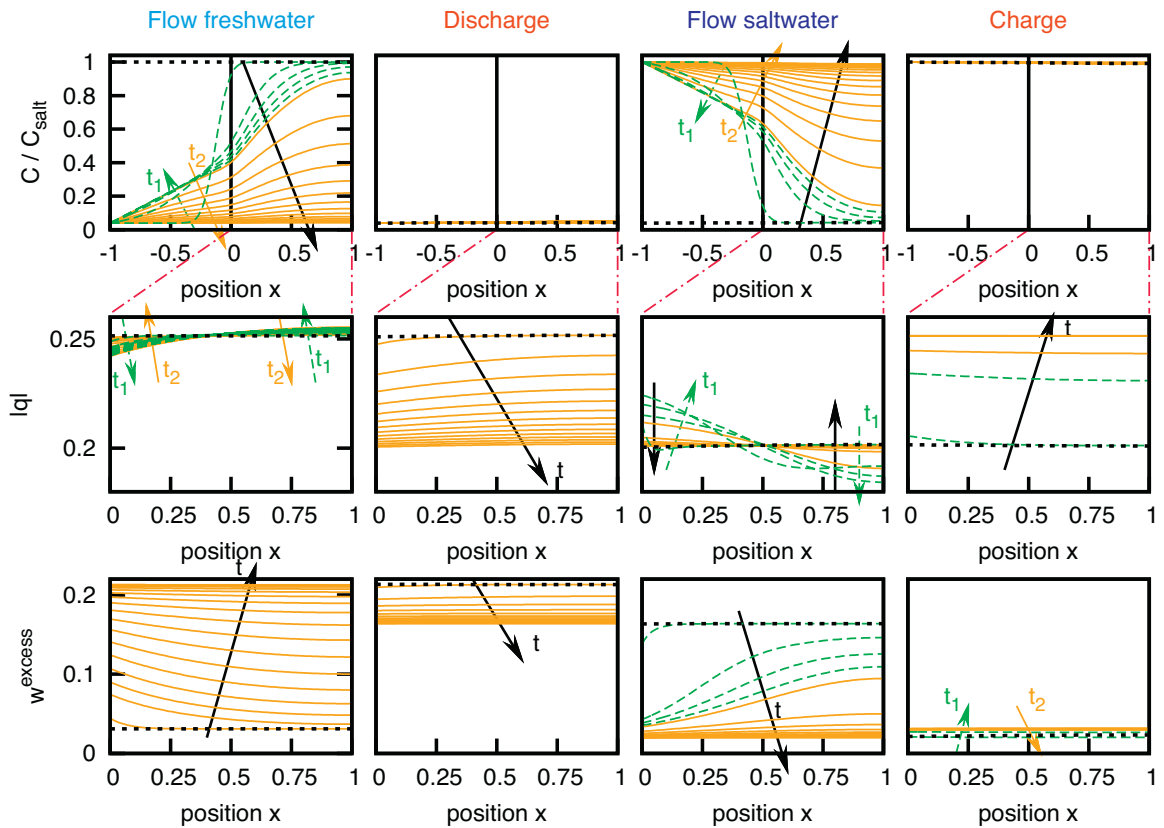


Fig. 6. Upper row: time evolution of salt concentration in the SDL ($x \in [-1, 0]$) and in the macropores inside the porous matrix ($x \in [0, 1]$). Middle and lower row: charge and salt adsorption, respectively, into the EDLs in the porous matrix ($x \in [0, 1]$, where adsorption takes place) as a function of the position x , in the four steps of the CAPMIX cycle in Fig. 4. Dashed green lines: $\Delta t = 1$ s. Solid orange lines: $\Delta t = 6$ s. Black dotted lines: initial condition at each step. Arrows indicate time evolution. (For interpretation of the references to color in this figure legend, the reader is referred to the web version of this article.)

its effects on the cell voltage, which is also influenced by the non-linear voltage–concentration dependence and the redistribution of charge discussed above.

Fig. 8 shows that the two different porosities work in opposite way: on the one hand, the larger the macroporosity the faster the electrode will respond to salinity changes, as the transport of salt is faster through larger paths for diffusion. On the other hand, the larger the microporosity is, the slower the response will be.

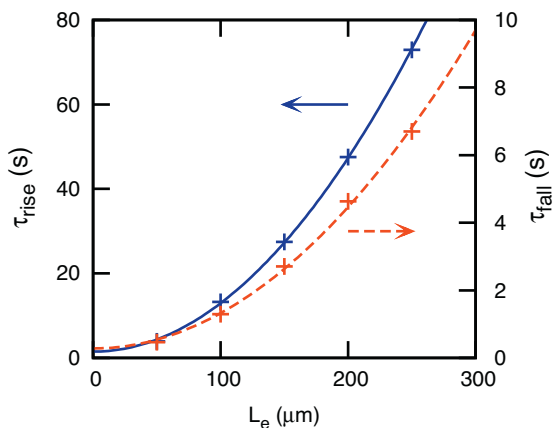


Fig. 7. Quadratic dependence of the characteristic rise and fall times with electrode thickness. Points: data obtained from simulations. Parameters: $A = 1.5 \text{ cm} \times 1.5 \text{ cm}$, $C_{\text{St,vol}} = 0.07 \text{ GF/m}^3$ and $p_{\text{mA}} = p_{\text{mi}} = 0.3$. Lines: best fits to a quadratic curve $\tau = \tau_0 + L_e^2/D_{\text{eff}}$. Best fit parameters: $\tau_0^{\text{rise}} = 1.5 \text{ s}$, $D_{\text{eff}}^{\text{rise}} = 8.7 \times 10^{-10} \text{ m}^2/\text{s}$; $\tau_0^{\text{fall}} = 0.3 \text{ s}$, $D_{\text{eff}}^{\text{fall}} = 9.7 \times 10^{-9} \text{ m}^2/\text{s}$.

However, a larger microporosity means a larger stored charge and energy generation. Therefore, there will be a compromise between a fast response and the energy extracted on each cycle to give the maximum power output. In general, we can say that large

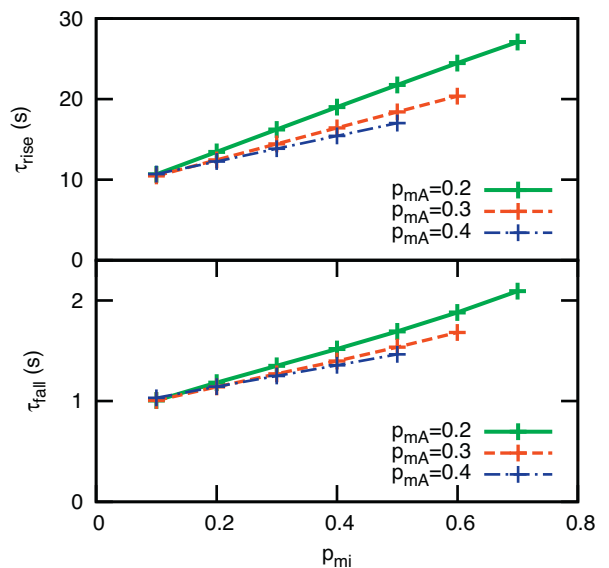


Fig. 8. Effect of macroporosity p_{mA} and microporosity p_{mi} on (a) the characteristic rise time (switch from salt to freshwater in open circuit) and (b) fall time (switch from fresh to saltwater in open circuit) of a CAPMIX cell. $A = 1.5 \text{ cm} \times 1.5 \text{ cm}$, $C_{\text{St,vol}} = 0.1 \text{ GF/m}^3$, $L_e = 100 \text{ μm}$.

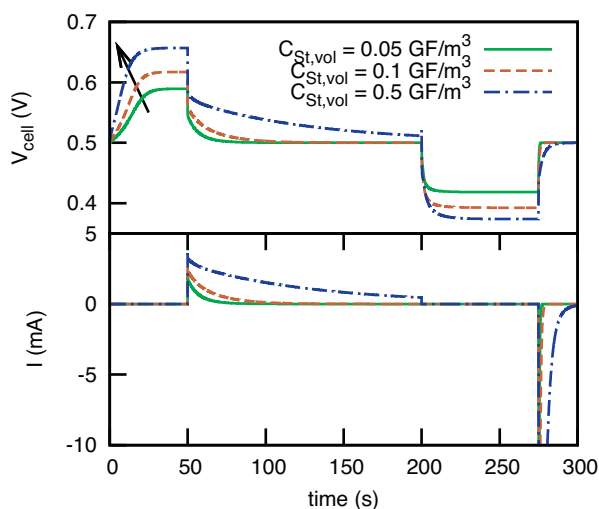


Fig. 9. Effect of the (volumetric) Stern layer capacitance on the performance of a CDLE CAPMIX cell. This plot shows that a larger value of $C_{St,vol}$ increases the stored charge, leads to a larger voltage rise and makes the cell respond faster to the solution change from salt to freshwater.

macroporosities are desirable, while the microporosity has to be carefully tuned.

The importance of the properties of the solid–liquid interface are depicted in Fig. 9, where we see that a larger Stern layer capacitance improves both the time response and the energy production. The specific capacitance of the interface depends for example on the hydrophilic/hydrophobic character of the material, being larger the more hydrophilic it is [59]. Inside the micropores,

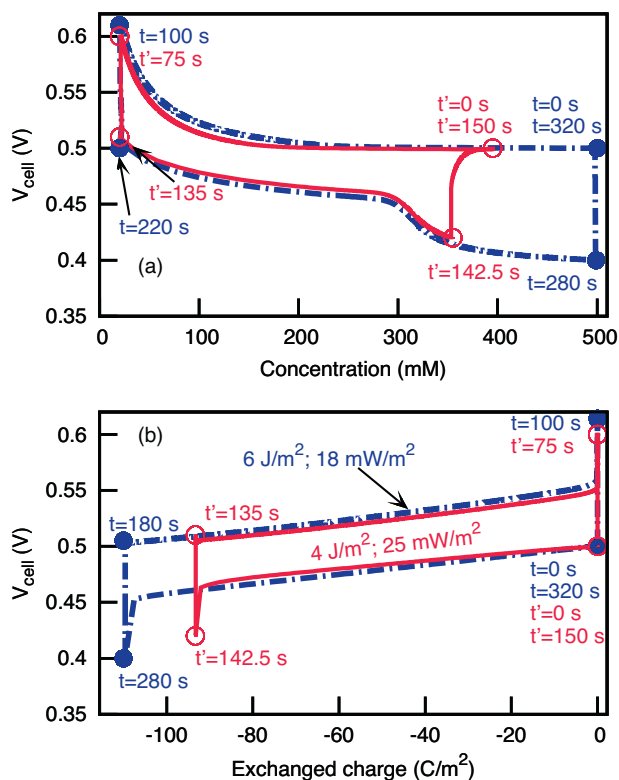


Fig. 10. A lower per-cycle energy production provides a larger power output, as illustrated in this comparison of the performance of the CAPMIX cycle shown in Figs. 1 and 5 with a shorter one, which does not allow to reach the maximum concentration at the interface between SDL and the porous matrix ($x=0$). Quantities with ' refer to the shorter cycle.

recent studies suggest a significant increase of the capacitance as the pore size is decreased (up to a limiting value, when the pore is smaller than the ion) [40,41], so smaller pores would be in general more desirable. However, it is not clear whether in the case of such small pores, when there is no room for the presence of a diffuse layer, the mechanism of CDLE can effectively take place.

Finally, Fig. 10 shows that an increase on power production can be obtained at the expense of a smaller energy extracted per cycle thanks to the non-linearity of the voltage–concentration dependence. As we already pointed out, the cell voltage depends very little on the salt concentration above $C \approx 350$ mM, and therefore it is not worth going beyond this value. In this way, the steps performed in saltwater can be done very fast with a small amount of lost energy. In the given example, we obtain an improvement of about 40% in power production, to which we must add the energy not consumed due to the decrease on pumping power demand.

4. Conclusions

In this work, we have studied for the first time the non-trivial kinetics of the CAPMIX technique to extract renewable energy from salinity differences. Our analysis takes into account the electrodiffusion of ions inside the porous matrix together with charge and salt adsorption into the EDLs formed at the solution/carbon interface. These adsorptions, whose rates depend on the EDL properties, can modify locally the salt concentrations, strongly affecting the kinetics of the process. Our treatment provides a full qualitative description of all the complex mechanisms affecting the performance of the CAPMIX cell. We have identified new transport phenomena and adsorption dynamics not described before. In particular, we have shown that the asymmetry in the open circuit phases of the CDLE cycle observed in experiments is due to the strongly non-linear dependence of the cell voltage on the salt concentration and to the non-uniform charge and salt adsorption established by redistribution currents inside each single electrode.

Finally, we have proposed guidelines for the optimal design of a CAPMIX cell, considering the engineering of materials, flow cells and appropriate cycle operation. Maximum power extraction is obtained with short cycles and large produced energy per cycle. We conclude that a fast time response requires thin electrodes and large macropores, while energy extraction is increased for small (sub-nanometer) micropores. Moreover, the maximum power production is not obtained if we allow the cell voltage to stabilize reaching a plateau, but if we only take advantage of the fast initial voltage rise.

Acknowledgements

Inspiring discussions with P.M. Biesheuvel (Wetsus, The Netherlands) and M.M. Fernández (University of Granada, Spain) are gratefully acknowledged. The research leading to these results received funding from the European Union Seventh Framework Programme (FP7/2007–2013) under agreement no. 256868. R.A.R. acknowledges support from Regione Lombardia (Accordo per lo sviluppo del capitale umano nel sistema universitario lombardo). F.M. and D.S. acknowledge support of Cariplo Foundation Materiali avanzati-2011, Project 2011-0336.

References

- [1] R.E. Pattle, Production of electric power by mixing fresh and salt water in the hydroelectric pile, *Nature* 174 (1954) 660.
- [2] O. Levenspiel, N. de Veuers, The osmotic pump, *Science* 183 (1974) 157.
- [3] R.S. Norman, Water salination: a source of energy, *Science* 186 (1974) 350.
- [4] S. Loeb, Osmotic power plant, *Science* 189 (1975) 654.
- [5] B.H. Clampitt, F.E. Kiviat, Energy recovery from saline water by means of electrochemical cells, *Science* 194 (1976) 719.

- [6] J.N. Weinstein, F.B. Leitz, Electric power from differences in salinity: the dialytic battery, *Science* 191 (1976) 557.
- [7] M. Olsson, G.L. Wick, J.D. Isaacs, Salinity gradient power: utilizing vapour pressure differences, *Science* 206 (1979) 452.
- [8] M.F.M. Bijmans, O.S. Burheim, M. Bryjak, A. Delgado, P. Hack, F. Mantegazza, S. Tennesson, H.V.M. Hamelers, Capmix-deploying capacitors for salt gradient power extraction, *Energy Procedia* 20 (2012) 108.
- [9] B. Logan, M. Elimelech, Membrane-based processes for sustainable power generation using water, *Nature* 488 (2012) 313.
- [10] T.-S. Chung, X. Li, R.C. Ong, Q. Ge, H. Wang, G. Han, Emerging forward osmosis (fo) technologies and challenges ahead for clean water and clean energy applications, *Current Opinion in Chemical Engineering* 1 (2012) 246.
- [11] J.W. Post, J. Veerman, H.V.M. Hamelers, G.J.W. Euverink, S.J. Metz, K. Nymeyer, C.J.N. Buisman, Salinity-gradient power: evaluation of pressure-retarded osmosis and reverse electrodialysis, *Journal of Membrane Science* 288 (2007) 218.
- [12] T. Thorsen, T. Holt, The potential for power production from salinity gradients by pressure retarded osmosis, *Journal of Membrane Science* 335 (2009) 103.
- [13] N.Y. Yip, M. Elimelech, Performance limiting effects in power generation from salinity gradients by pressure retarded osmosis, *Environmental Science and Technology* 45 (2011) 10273.
- [14] J.W. Post, H.V.M. Hamelers, C.J.N. Buisman, Energy recovery from controlled mixing salt and fresh water with a reverse electrodialysis system, *Environmental Science and Technology* 42 (2008) 5785.
- [15] J. Veerman, M. Saakes, S. Metz, G. Harmsen, Reverse electrodialysis: performance of a stack with 50 cells on the mixing of sea and river water, *Journal of Membrane Science* 327 (2009) 136.
- [16] P. Dlugolecki, A. Gambier, K. Nijmeijer, M. Wessling, Practical potential of reverse electrodialysis as process for sustainable energy generation, *Environmental Science and Technology* 43 (2009) 6888.
- [17] M.B. Andersen, M. van Soestbergen, A. Mani, H. Bruus, P.M. Biesheuvel, M.Z. Bazant, Current-induced membrane discharge, *Physical Review Letters* 109 (2012) 108301.
- [18] B. Conway, *Electrochemical Supercapacitors*, Kluwer Academic, Plenum Publishers, London, 1999.
- [19] R. Kötz, M. Carlen, Principles and applications of electrochemical capacitors, *Electrochimica Acta* 45 (2000) 2483.
- [20] P. Simon, Y. Gogotsi, Materials for electrochemical capacitors, *Nature Materials* 7 (2008) 845.
- [21] D. Brogioli, Extracting renewable energy from a salinity difference using a capacitor, *Physical Review Letters* 103 (2009) 058501.
- [22] J. Veerman, M. Saakes, S. Metz, G. Harmsen, Reverse electrodialysis: evaluation of suitable electrode systems, *Journal of Applied Electrochemistry* 40 (2010) 1461, cited by (since 1996) 10.
- [23] D. Brogioli, R. Zhao, P.M. Biesheuvel, A prototype cell for extracting energy from a water salinity difference by means of double layer expansion in nanoporous carbon electrodes, *Energy & Environmental Science* 4 (2011) 772.
- [24] B.B. Sales, M. Saakes, J. Post, C.J.N. Buisman, P.M. Biesheuvel, H.V.M. Hamelers, Direct power production from a water salinity difference in a membrane-modified supercapacitor flow cell, *Environmental Science and Technology* 44 (2010) 5661.
- [25] F. Liu, O. Schaetzle, B.B. Sales, M. Saakes, C.J.N. Buisman, H.V.M. Hamelers, Effect of additional charging and current density on the performance of capacitive energy extraction based on Donnan potential, *Energy & Environmental Science* 5 (2012) 8642.
- [26] W. Guo, L. Cao, J. Xia, F.-Q. Nie, W. Ma, J. Xue, Y. Song, D. Zhu, Y. Wang, L. Jiang, Energy harvesting with single-ion-selective nanopores: a concentration-gradient-driven nanofluidic power source, *Advanced Functional Materials* 20 (2010) 1339.
- [27] F. La Mantia, M. Pasta, H.D. Deshazer, B.E. Logan, Y. Cui, Batteries for efficient energy extraction from a water salinity difference, *Nano Letters* 11 (2011) 1810.
- [28] Y. Oren, Capacitive deionization (CDI) for desalination and water treatment – past, present and future (a review), *Desalination* 228 (2008) 10.
- [29] S. Porada, L. Weinstein, R. Dash, A. Van Der Wal, M. Bryjak, Y. Gogotsi, P. Biesheuvel, Water desalination using capacitive deionization with microporous carbon electrodes, *ACS Applied Materials & Interfaces* 4 (2012) 1194.
- [30] P.M. Biesheuvel, Thermodynamic cycle analysis for capacitive deionization, *Journal of Colloid and Interface Science* 332 (2009) 258.
- [31] N. Boon, R. van Rooij, 'Blue energy' from ion adsorption and electrode charging in sea and river water, *Molecular Physics* 109 (2011) 1229.
- [32] R.A. Rica, R. Ziano, D. Salerno, F. Mantegazza, D. Brogioli, Thermodynamic relation between voltage–concentration dependence and salt adsorption in electrochemical cells, *Physical Review Letters* 109 (2012) 156103.
- [33] D. Brogioli, R. Ziano, R.A. Rica, D. Salerno, O. Kozynchenko, H.V.M. Hamelers, F. Mantegazza, Exploiting the spontaneous potential of the electrodes used in the capacitive mixing technique for the extraction of energy from salinity difference, *Energy & Environmental Science* 5 (2012) 9870.
- [34] K. Hess, W. Epting, S. Litster, Spatially resolved, in situ potential measurements through porous electrodes as applied to fuel cells, *Analytical Chemistry* 83 (2011) 9492.
- [35] K.C. Hess, J.F. Whitacre, S. Litster, In situ measurements of potential, current and charging current across an EDL capacitance anode for an aqueous sodium hybrid battery, *Journal of the Electrochemical Society* 159 (2012) A1351.
- [36] R.A. Rica, D. Brogioli, R. Ziano, D. Salerno, F. Mantegazza, Ion transport and adsorption mechanisms in porous electrodes during capacitive–mixing double layer expansion (CDLE), *Journal of Physical Chemistry C* 116 (2012) 16934.
- [37] J. Lyklema, *Fundamentals of Interface and Colloid Science*, vol. 2, Academic, New York, 1995.
- [38] F. Carrique, F.J. Arroyo, A.V. Delgado, Electrokinetics of concentrated suspensions of spherical colloidal particles with surface conductance, arbitrary zeta potential, and double-layer thickness in static electric fields, *Journal of Colloid and Interface Science* 252 (2002) 126.
- [39] M.L. Jimenez, M.M. Fernandez, S.A. Ahualli, G.R. Iglesias, A.V. Delgado, Realistic predictions of energy extraction from salinity differences inside porous electrodes, *Environmental Science and Technology*, Under review.
- [40] J. Chmiola, G. Yushin, Y. Gogotsi, C. Portet, P. Simon, P.L. Taberna, Anomalous increase in carbon capacitance at pore sizes less than 1 nanometer, *Science* 313 (2006) 1760.
- [41] C. Merlet, B. Rotenberg, P.A. Madden, P. Taberna, P. Simon, Y. Gogotsi, M. Salanne, On the molecular origin of supercapacitance in nanoporous carbon electrodes, *Nature Materials* 11 (2012) 306.
- [42] D. Jiang, Z. Jin, J. Wu, Oscillation of capacitance inside nanopores, *Nano Letters* 11 (2011) 5373.
- [43] D. Henderson, Oscillations in the capacitance of a nanopore containing an electrolyte due to pore width and nonzero size ions, *Journal of Colloid and Interface Science* 374 (2012) 345.
- [44] D. Jiang, Z. Jin, D. Henderson, J. Wu, Solvent effect on the pore-size dependence of an organic electrolyte supercapacitor, *Journal of Physical Chemistry Letters* 3 (2012) 1727.
- [45] P. Wu, J. Huang, V. Meunier, B.G. Sumpter, R. Qiao, Voltage dependent charge storage modes and capacity in subnanometer pores, *Journal of Physical Chemistry Letters* 3 (2012) 1732.
- [46] J.J. Bikerman, Structure and capacity of electrical double layer, *Philosophical Magazine* 33 (1942) 384.
- [47] I. Borukhov, D. Andelman, H. Orland, Steric effects in electrolytes: a modified Poisson–Boltzmann equation, *Physical Review Letters* 79 (1997) 435.
- [48] A. Kornyshev, Double-layer in ionic liquids: paradigm change? *Journal of Physical Chemistry B* 111 (2007) 5545.
- [49] M.Z. Bazant, M.S. Kilic, B.D. Storey, A. Ajdari, Towards an understanding of induced-charge electrokinetics at large applied voltages in concentrated solutions, *Advances in Colloid and Interface Science* 152 (2009) 48.
- [50] H. Wang, L. Pilon, Accurate simulations of electric double layer capacitance of ultramicroelectrodes, *Journal of Physical Chemistry C* 115 (2011) 16711.
- [51] M. Bazant, B. Storey, A. Kornyshev, Double layer in ionic liquids: overscreening versus crowding, *Physical Review Letters* 106 (2011) 046102.
- [52] P.M. Biesheuvel, M.Z. Bazant, Nonlinear dynamics of capacitive charging and desalination by porous electrodes, *Physical Review E: Statistical, Nonlinear, and Soft Matter Physics* 81 (2010) 031502.
- [53] B.B. Sales, O.S. Burheim, F. Liu, O. Schaetzle, C.J. Buisman, H.V. Hamelers, Impact of wire geometry in energy extraction from salinity differences using capacitive technology, *Environmental Science and Technology* 46 (2012) 12203.
- [54] O.S. Burheim, F. Liu, B.B. Sales, O. Schaetzle, C.J.N. Buisman, H.V.M. Hamelers, Faster time response by the use of wire electrodes in capacitive salinity gradient energy systems, *Journal of Physical Chemistry C* 116 (2012) 19203.
- [55] S. Porada, B.B. Sales, H.V.M. Hamelers, P.M. Biesheuvel, Water desalination with wires, *Journal of Physical Chemistry Letters* 3 (2012) 1613.
- [56] M.E. Suss, T.F. Baumann, W.L. Bourcier, C.M. Spadaccini, K.A. Rose, J.G. Santiago, M. Stadermann, Capacitive desalination with flow-through electrodes, *Energy & Environmental Science* 5 (2012) 9511.
- [57] P.M. Biesheuvel, Y. Fu, M.Z. Bazant, Diffuse charge and faradaic reactions in porous electrodes, *Physical Review E: Statistical, Nonlinear, and Soft Matter Physics* 83 (2011) 061507.
- [58] M.M. Hatlo, R. van Rooij, L. Lue, The electric double layer at high surface potentials: the influence of excess ion polarizability, *Europhysics Letters (EPL)* 97 (2012) 28010.
- [59] D.J. Bonthuis, S. Gekle, R.R. Netz, Dielectric profile of interfacial water and its effect on double-layer capacitance, *Physical Review Letters* 107 (2011) 166102.
- [60] A. Revil, N. Linde, Chemico-electromechanical coupling in microporous media, *Journal of Colloid and Interface Science* 302 (2006) 682.
- [61] M. Murad, C. Moyné, A dual-porosity model for ionic solute transport in expansive clays, *Computers & Geosciences* 12 (2008) 47.
- [62] P.M. Biesheuvel, R. Zhao, S. Porada, A. van der Wal, Theory of membrane capacitive deionization including the effect of the electrode pore space, *Journal of Colloid and Interface Science* 360 (2011) 239.
- [63] M.Z. Bazant, K. Thornton, A. Ajdari, Diffuse-charge dynamics in electrochemical systems, *Physical Review E: Statistical, Nonlinear, and Soft Matter Physics* 70 (2004) 021506.
- [64] A. Delgado, F. Gonzalez-Caballero, R. Hunter, L. Koopal, J. Lyklema, Measurement and interpretation of electrokinetic phenomena, *Journal of Colloid and Interface Science* 309 (2007) 194.
- [65] S. Ahualli, A. Delgado, S. Miklavcic, L. White, Dynamic electrophoretic mobility of concentrated dispersions of spherical colloidal particles on the consistent use of the cell model, *Langmuir* 22 (2006) 7041.
- [66] R. Roa, F. Carrique, E. Ruiz-Reina, Ion size effects on the electric double layer of a spherical particle in a realistic salt-free concentrated suspension, *Physical Chemistry Chemical Physics* 13 (2011) 9644.

- [67] B. Kastening, M. Heins, Properties of electrolytes in the micropores of activated carbon, *Electrochimica Acta* 50 (2005) 2487.
- [68] M. Levi, G. Salitra, N. Levy, D. Aurbach, J. Maier, Application of a quartz-crystal microbalance to measure ionic fluxes in microporous carbons for energy storage, *Nature Materials* 8 (2009) 872.
- [69] M. Kaus, J. Kowal, D. Sauer, Modelling the effects of charge redistribution during self-discharge of supercapacitors, *Electrochimica Acta* 55 (2010) 7516.
- [70] R. Zhao, M. van Soestbergen, H. Rijnaarts, A. van der Wal, M. Bazant, P. Biesheuvel, Time-dependent ion selectivity in capacitive charging of porous electrodes, *Journal of Colloid and Interface Science* 384 (2012) 38.
- [71] R. Zhao, P.M. Biesheuvel, H. Miedema, H. Bruning, A. van der Wal, Charge efficiency: a functional tool to probe the double-layer structure inside of porous electrodes and application in the modeling of capacitive deionization, *Journal of Physical Chemistry Letters* 1 (2010) 205.